Infrared and Laser Spectroscopic Characterization of Aluminum Defects in Cultured Quartz

HERBERT G. LIPSON

Abstract—**Optical absorption at He-Ne and argon laser frequencies has been used to map the distribution of aluminum-hole centers, Al-h^+, in irradiated and vacuum swept quartz. The absorption band associated with Al-h^+ has a strong peak centered at 435 nm and a weaker one at 633 nm. Argon laser lines at 488 and 514.5 nm are close to the wavelength of the stronger peak while the He-Ne line at 632.8 nm is nearly coincident with that of the weaker peak. Large variations in Al-h^+ absorption for irradiated and vacuum swept crystals correspond to visually observed changes in coloration. The laser method is sensitive and nondestructive and gives a quantitative measurement adaptable to computerized scanning and recording of data. Measurements of both Al-h^+ and infrared-active aluminum hydroxide centers, Al-OH^-, are used to evaluate the distribution of aluminum-associated defect centers and determine aluminum variations over an entire crystal.**

Introduction

THE PRINCIPAL GROWTH DEFECTS in quartz involved in irradiation and sweeping (electrodiffusion) are as-grown OH^-, formed by a hydrogen ion adjacent to an oxygen site and those associated with aluminum substitutional in a silicon site. These defects and their characterization techniques are reviewed in several publications [1]–[7]. Ionizing radiation dissociates the aluminum metal center Al-M^+(M = Li, Na) and Al^{3+} is compensated either with hydrogen from OH^- in the crystal to form Al-OH^-, or with a hole trapped at a non-bonding oxygen ion to form an aluminum-hole center $[AlO_4]^0$, designated here as Al-h^+. Steady-state and transient frequency offsets from irradiation-induced changes can occur in oscillators that employ resonators fabricated from quartz containing aluminum impurities [8], [9]. Sweeping also dissociates Al-M^+, but in this case most of the alkalis are removed from the crystal rather than being displaced to another site. Sweeping in air introduces additional hydrogen for Al^{3+} compensation and forms only Al-OH^-. Sweeping in a vacuum produces either Al-OH^- or Al-h^+ or both.

As-grown OH^- and aluminum concentrations can vary considerably across a single bar used for resonator fabrication. Nondestructive techniques are required to determine the concentration and distribution of these impurities and associated defect centers, before and after irradiation and sweeping. We previously reported the application of low-temperature Fourier spectroscopy to sensitively monitor changes in hydrogen-related absorption bands in as-grown and swept quartz [10]–[12]. We have also reported the irradiation dose dependence of the hydrogen-related centers [13]. The aluminum profile across a sample can be determined from the Al-OH^- distribution after irradiation to saturation in cases where all aluminum is compensated with hydrogen [14]. Sweeping the sample in air can restore OH^- when depleted [15]. In cases where air sweeping is impractical, or with vacuum sweeping, a similar method for determining Al-h^+ distribution is necessary. Al-h^+ can be measured by electron spin resonance (ESR) [5], [6], and aluminum concentrations deduced, but this technique requires that many small samples be cut from the region to be examined and is therefore not easily applicable to nondestructive evaluation. Visible coloration of irradiated quartz is a well-known phenomenon and absorption bands in this spectral region and their relation to aluminum content and Al-h^+ centers have been extensively investigated [16]–[20]. Optically detected magnetic resonance measurements at 1.6 K by Meyer *et al.* [21] have shown that the A_3 band associated with Al-h^+ has a strong peak at 2.85 eV (436 nm) and a weaker one at 1.96 eV (633 nm). While conventional visible spectroscopy can be used to determine Al-h^+ absorption bands, most instruments do not provide the nearly parallel beam optics necessary to accurately measure localized variations in transmission of relatively thick samples. The small diameter, high intensity, monochromatic beams of lasers are better adapted to scanning crystals for localized impurity or defect absorption. Argon laser lines at 488.0 and 514.5 nm are close to the wavelength of the stronger A_3 peak and the He-Ne laser line at 632.8 nm is nearly coincident with that of the weaker peak. Thus either of these lasers should be useful for scanning quartz samples for Al-h^+ absorption [22], [23]. Absorption obtained with argon lines will include a background whose main contribution is the A_2 band that peaks at 2.33 eV (532 nm), while the main background contribution with the He-Ne line is the A_1 band that peaks at 1.77 eV (700 nm). In this paper absorption at laser frequencies is used to map the distribution of Al-h^+ centers in irradiated and vacuum swept quartz. A calibration of 632.8 nm absorption strength versus Al-h^+ concentration is made using the ESR value obtained for the same

Manuscript received July 10, 1989; revised December 7, 1989; accepted April 13, 1990.

The author was with Rome Air Development Center, Solid State Sciences Directorate, Hanscom AFB, MA 01731-5000. He is now at 68 Aldrich Rd., Wakefield, MA 01880.

IEEE Log Number 903827.

section of a vacuum swept sample. Aluminum variations are determined from the combination of infrared Al-OH^- and laser Al-h^+ measurements.

Experimental Procedures

The quartz samples used for this investigation were rectangular in shape, between 1 and 4 cm in size, with parallel x, y, and z faces. Premium-Q samples H29-14 and BH-A were grown by Sawyer Research Products (SARP). QA-32 and QA-38 were grown at Rome Air Development Center (RADC) from nutrients of recrystallized glass and z-growth quartz, respectively. One of the samples, H29-14, was air swept by SARP. Sweeping in a vacuum atmosphere at 10^{-5} Torr was performed at RADC at 500°C with electric fields of 1000 to 1500 V/cm. Al-h^+ and aluminum concentrations for the samples were measured by ESR from 2.5 × 2.5 × 8 mm sections.[1] Samples were irradiated to saturation in the RADC ^{60}Co source at doses up to 4 Mrad (Si). The irradiation temperature was a few degrees above room temperature.

Infrared transmissions were measured between 3100 and 3700 cm^{-1} with the unpolarized focused beam of a Nicolet 170SX spectrometer at 2 cm^{-1} resolution. Either a 1.5 or 3 mm beam diameter was used with overlapping scans taken at 1 or 2 mm intervals. The infrared measurement method, OH^- and Al-OH^- band spectra, and the dependence of absorption of these bands on temperature, crystal direction and polarization are described in previous papers [10]–[12]. For these measurements, the sample positioned inside a Dewar cooled to 85K, was scanned along the z-axis with the infrared beam directed along the crystal x- or y-axis. The peak absorptions of the strong narrow bands at 3581 cm^{-1} and 3366 cm^{-1} are selected to monitor relative changes in as-grown OH^- and Al-OH^-, respectively.

The overall absorption of a 5 × 10 mm section of each sample was measured between 320 and 800 nm at room temperature on a Cary 14 spectrometer, using unpolarized light. Absorption variations across the sample were determined from laser scans made at a rate of 2 mm/min. A comparison of the absorption levels and polarization dependence for 488.0 nm argon and 632.8 nm He-Ne laser wavelengths was made. For these comparative measurements the lasers were operated at power levels of 2 to 4 mW with 488.0 nm and 632.8 nm beam diameters of 1.5 and 0.67 nm, respectively. A broad band rotary polarizer and polarizing analyzer were used to rotate and adjust the plane of polarization. Most of the absorption measurements were made with an unfocused, randomly polarized, low power He-Ne laser, 0.15 mW as measured by a silicon detector, chosen on the basis of convenience and stability. The laser beam, with a diameter of 0.88 mm at $1/e^2$ was propagated parallel to the crystal x- or y-axis and the sample scanned along the z-axis. For one of the samples the beam was focused to about 0.2 mm to study strongly varying regions in more detail.

Experimental Results and Discussion

Room temperature absorption between 320 and 770 nm is shown in Fig. 1 for sample E42-21, which was vacuum swept for 8 days. The section selected for measurement contained the darkest colored regions of the sample shown in the photograph of Fig. 2(b). Aluminum concentrations of 6 to 8 ppm were determined for other sections of this sample by ESR. This spectrum is a composite of overlapping broad A_1, A_2, A_3, and B absorption bands, and has relatively strong absorption at argon and He-Ne laser wavelengths.

Fig. 2(a) shows variations in 632.8 nm He-Ne laser transmission observed along the z- or sweeping axis, between the anode ($+z$-face) and cathode ($-z$-face) of vacuum swept sample E42-21. Transmission scans were made for 15 x-axis positions with the beam directed along the y-axis and focused to about 0.2 mm. The transmission can be compared with the visible coloration for each of these positions indicated in the photograph of Fig. 2(b). The largest decrease in transmission, a 43% reduction measured at position 14, is for the darkest region of the sample and corresponds to a 632.8-nm absorption value of 1.4 cm^{-1}. Good correspondence between major dips in transmission and the degree of darkening of other sections of the crystal is found. Some small variations in transmission not observed when the beam was defocused are attributed to interference effects. Thus absorption at the laser wavelength can be used as a quantitative measure of crystal coloration. The Al-h^+ variations observed from 632.8 nm absorption are an indication of strongly varying aluminum in this sample.

Absorption spectra obtained with argon and He-Ne lasers using different polarizations are compared in Fig. 3. The sample, a 3.2 Mrad irradiated section of sample QA-32, containing a $+x$-growth region, was scanned across the z-axis at the x-axis beam position indicated in the photograph of Fig. 3. No absorption data was taken between 0 and 2 mm where a crack in the sample developed. All spectra show a sharp rise, decrease to a minimum and subsequent rise as the beam traverses the clear z-growth and colored s- and $+x$-growth regions. The high absorption levels at both the He-Ne and argon laser wavelengths demonstrate that either laser can be used to measure variations in Al-h^+ concentration in this sample with good sensitivity. The overall absorption is a factor of 1.5–1.7 higher for the 488.0-nm argon line relative to the 632.8-nm He-Ne line. Some differences between argon and He-Ne spectra may be due to the different beam sizes of the lasers, 1.5 mm for argon and 0.67 mm for He-Ne. Contributions from the underlying A_1 band whose peak (700 nm) is close to the 632.8 nm He-Ne wavelength and the A_2 band whose peak (532 nm) is close to the 488.0-nm argon wavelength may also introduce differences. The strongest absorption is observed with polarization parallel to the z-axis (π-spectra) and the weakest with polariza-

[1]All ESR measurements for this investigation were performed by L. Halliburton at Oklahoma State University.

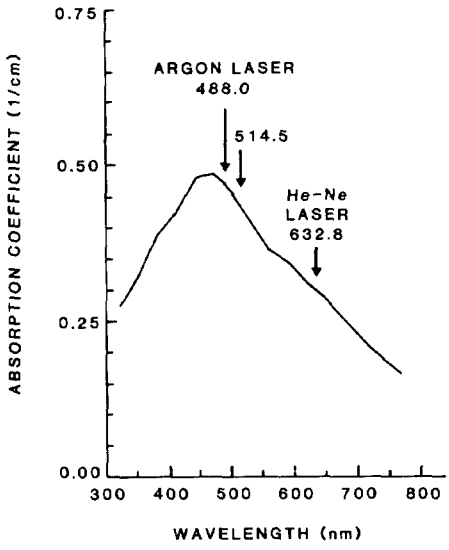

Fig. 1. Room temperature optical absorption of sample E42-21 after vacuum sweeping for 8 days. Wavelength positions of principal argon and He-Ne laser lines are indicated.

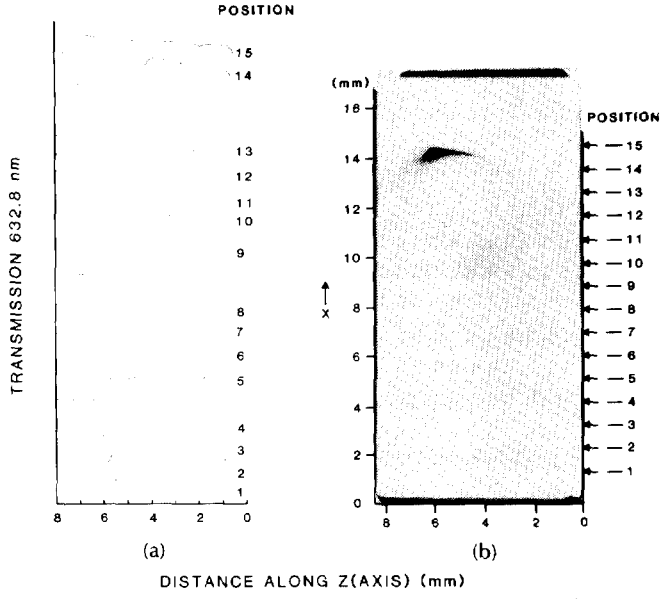

Fig. 2. Comparison of (a) room temperature 632.8 nm He-Ne laser transmission obtained from scans between the $+z$ and $-z$-faces at the 15 different x-positions indicated in (b) with coloration of sample E42-21 after vacuum sweeping for 8 days. Transmission spectra are displaced for clarity.

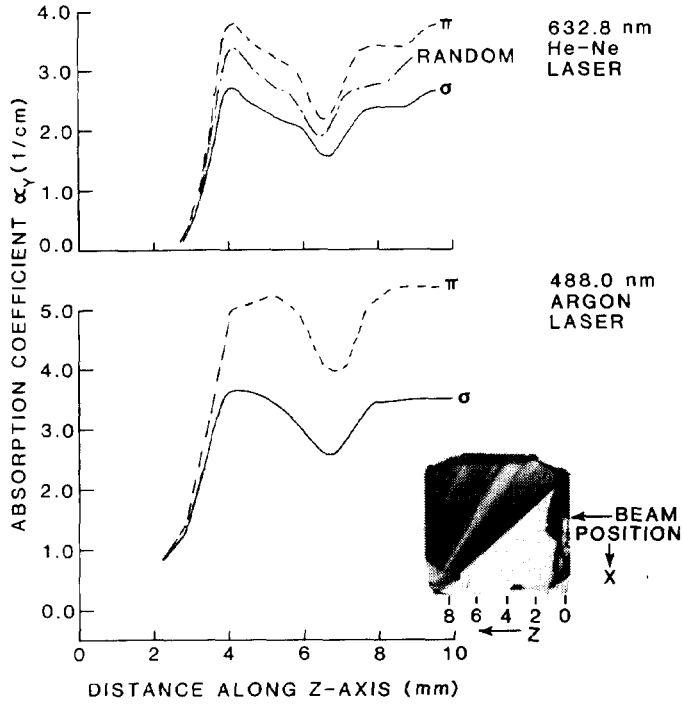

Fig. 3. Room temperature absorption coefficient values α_y obtained for scan along the z-axis of sample QA-32 after a 3.2 Mrad ^{60}Co irradiation. Laser beam whose x-position is indicated by arrow in insert traverses z-, s-, and $+x$-growth regions. Results of measurements with a 632.8 nm He-Ne laser, polarized randomly, perpendicular (σ-spectra) and parallel (π-spectra) to the sample z-axis, and those obtained with a 488.0 nm argon laser, perpendicular (σ) and parallel (π) to z-axis, are shown.

tion and the relation α_y 3366 cm^{-1}/(0.17 ± 0.04) = Al ppm [14], a rough estimate of 6 ppm Al are compensated with hydrogen. The combination gives an Al concentration variation of 23 to 37 ppm. The Al concentration determined from a single ESR sample cut from the dark colored $+x$-growth region was 32 ppm.

Fig. 4(a) shows 632.8 nm Al-h$^+$ absorption and Fig. 4(b) shows 3581 cm^{-1} OH$^-$ and 3366 cm^{-1} Al-OH$^-$ absorption for positions 1, 2, and 3, located 5, 19, and 32 mm from the $-y$ face of sample H29-14. This sample was initially air swept and then vacuum swept. Although the combination of air sweeping and vacuum sweeping at fields up to 1500 V/cm in successive stages for a total of 52 days failed to remove all hydrogen from this sample, tion perpendicular to the z-axis (σ-spectra), an average π/σ ratio of 1.51 for 488.0 nm and 1.42 for 632.8 nm. Intermediate absorption values are observed with a randomly polarized laser.

A calibration of 0.1 cm^{-1}/ppm Al-h$^+$ for 632.8 nm absorption was previously determined for a sample from ESR measurements [23]. A check on this value was made using a vacuum swept sample of BH-A in which Al-h$^+$ was produced. An average 632.8 nm absorption value of 0.034 cm-1 was measured over the same region of the sample for which a 0.42 ppm Al-h$^+$ concentration was determined by ESR, leading to a calibration of 0.08 cm^{-1}/ppm Al-h$^+$. Considering the possible sources of error in both absorption and ESR measurements as well as nonuniformities in the Al-h$^+$ distribution, these values are in reasonable agreement and an average value of 0.09 ± 0.01 cm^{-1}/ppm is used for Al-h$^+$ concentration. The randomly polarized 632.8 nm He-Ne absorption range of sample QA-32 of Fig. 3 gives an Al-h$^+$ variation of 17 to 31 ppm. The 3.2 Mrad irradiation was sufficient to deplete OH$^-$ and saturate Al-OH$^-$. From the average 3366 cm^{-1} Al-OH$^-$ absorption measured for this crystal sec- some regions were depleted of OH$^-$ and changes in the Al-OH$^-$ distribution were effected [11]. The Al-h$^+$ distribution and its relation to the hydrogen-compensated centers is of interest here.

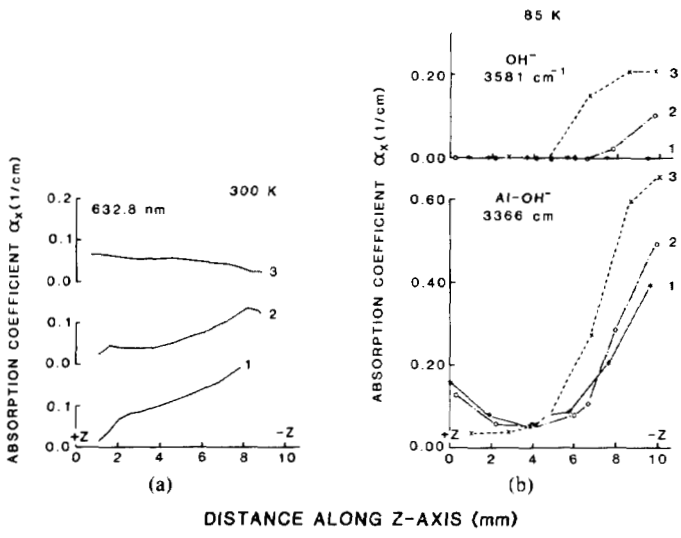

Fig. 4. (a) 632.8 nm and (b) 3366 cm^{-1} and 3581 cm^{-1} band peak absorption coefficient values α_x measured along the z-axis at three different y-positions for sample H29-14 after air sweeping and 52 days of vacuum sweeping. Positions 1, 2, and 3, were located 5, 19, and 32 mm from the $-y$ face, respectively, for this 36-mm-long sample section.

After air sweeping, OH^- varied from 2 to 3 ppm and Al-OH^- from 3 to 4 ppm between the anode ($+z$-face) and cathode ($-z$-face), as determined from the OH^- absorption/concentration relations of Kats [1], corrected for our spectrometer polarization and resolution, and the Al-OH^-/Al concentration relation of [14]. Vacuum sweeping depleted OH^- in region 1 and depleted or reduced OH^- in regions 2 and 3. For all regions, Al-OH^- was reduced to less than 1 ppm near the center of the sample and then increased sharply between the center and the cathode, with the highest concentration close to the cathode.

While variations in coloration were hard to distinguish for this sample, 632.8 nm absorption shows Al-h^+ formation in most of the regions where OH^- was depleted or reduced. In region 3, where little Al-OH^- is found near the anode, Al-h^+ is higher near the anode and decreases toward the cathode, where a large OH^- concentration still remains. Regions 1 and 2 show little Al-h^+ formation close to the anode, where Al-OH^- is higher than at the center. This unexpected result is attributed to sweeping in of hydrogen impurities present on the crystal surface or electrode. Al-h^+ increases toward the cathode beyond the 2-mm z-position for these regions. In this incompletely vacuum swept sample, Al-OH^- and Al-h^+ coexist with Al-OH^- dominating in regions containing the most remanent OH^-. The increase in both types of aluminum-compensating defects toward the $-z$-face is an indication of higher Al concentration in this part of the crystal. ESR measurements give 2.4–2.5 ppm Al for samples taken adjacent to the $+z$-face and 5.5–7.5 ppm for samples taken adjacent to the $-z$-face.

The z-growth sections of cultured quartz are customarily used for resonator manufacture, but bordering $-x$-growth regions that contain high OH^- or aluminum concentrations are occasionally accidentally included in the cut. The seed and z- and $-x$-growth regions are usually delineated from the coloration produced by irradiation. The 632.8-nm absorption and infrared scans are used to examine the aluminum distribution and the type of compensation in z- and $-x$-growth regions of low aluminum sample QA-38. An average of 0.5 ppm Al was measured by ESR for the z-growth region of this crystal. Fig. 5 shows (a) the coloration, (b) 632.8 nm Al-h^+, (c) 3581 cm^{-1} OH^-, and (d) 3366 cm^{-1} Al-OH^- absorption obtained from scans along the z-axis after a 2 Mrad ^{60}Co irradiation. The size and x-axis position for the infrared beam are indicated by the circles of Fig. 5(a), while the x-axis laser beam positions are designated at the right of Fig. 5(b). The dashed lines of Fig. 5(a) give the scanning direction.

The outline of the seed and $-x$-growth region can be seen from the dark colored areas in the center of Fig. 5(a). The darkened lines close to the left edge of the photograph are reflections from the back surface of the sample. The absorption measured at the various x-positions gives a good mapping of the Al-h^+ centers responsible for the coloration. The 632.8-nm absorption is strongest in the seed and bordering $-x$-growth regions and decreases rapidly with distance from the seed. At the 10.5 mm $-x$-position the absorption value is 0.05 to 0.06 cm^{-1}, not much higher than the average 0.04 cm^{-1} level found in the z-growth sections.

Fig. 5(c) shows that the 2 Mrad ^{60}Co irradiation dose markedly reduces or depletes OH^- in the seed and z-growth regions. High concentrations of OH^- still remain in the $-x$-growth region, increasing and becoming more uniform with distance from the seed. From a comparison of Figs. 5(c) and 5(d) it can be seen that the Al-OH^- profile follows the OH^- distribution across the crystal, except for the seed. The highest Al-OH^- and Al-h^+ absorptions are at the border of the seed and $-x$-growth region, where both aluminum and OH^- concentrations are high.

Conclusion

In a radiation environment steady-state and transient frequency offsets occur in oscillators fabricated from quartz containing aluminum impurities. Laser absorption is a useful nondestructive method for observing aluminum hole, Al-h^+, defects in irradiated quartz containing aluminum impurities and can aid in material selection. Although Al-h^+ absorption is stronger with either the 488.0 or 514.5 nm line of an argon laser, adequate sensitivity for mapping this defect in quartz is obtained with the 632.8 nm line of more convenient low power He-Ne lasers. After alkalis are displaced by irradiation or removed by sweeping, the aluminum center is compensated by the formation of either Al-h^+ or infrared-active Al-OH^-. The combination of laser and infrared scans provides information on the type of aluminum compensation present in each region of the crystal and can be used to determine the aluminum distribution.

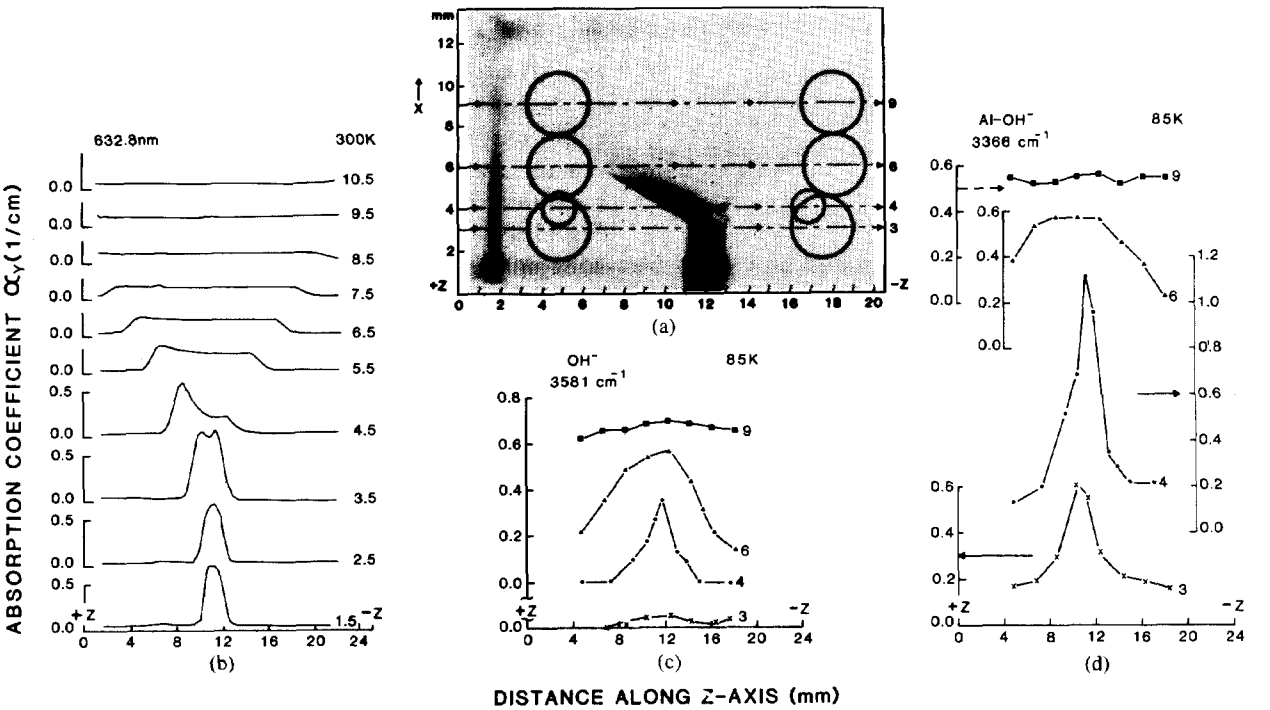

Fig. 5. (a) Coloration, (b) 632.8 nm, and (c) 3581 cm^{-1} and (d) 3366 cm^{-1} band peak absorption coefficient values α_y as a function of position along the z-axis for $-x$ and z-growth regions of sample QA-38 after a 2 Mrad ^{60}Co irradiation. Diameter of infrared beam and the positions along the x-axis of the crystal at which measurements were taken are shown in Fig. 5(a). Measurement positions for the 632.8 nm beam are shown in Fig. 5(b).

The results of this investigation indicate that both forms of compensation co-exist, with Al-OH^- dominating in regions still containing high remanent OH^-. Al-h^+ concentration increases when irradiation, or vacuum sweeping, reduces or depletes OH^-. Changes in Al-h^+ and Al-OH^- distributions can also be used to monitor the progress of vacuum sweeping.

Acknowledgment

The author would like to thank his co-workers at RADC for their contributions to this paper, A. Kahan, F. Euler, and P. Zecchini, visiting scientist from the University of Besançon, for many helpful discussions, A. Armington and M. T. Harris for performing the sweeping experiments, J. Schott for the sample irradiation, and R. Andrews for assistance in performing measurements and data reduction. He would also like to express his appreciation to Professor L. Halliburton of Oklahoma State University for helpful discussions on interpreting electron spin resonance results.

References

[1] A. Kats, "Hydrogen in alpha-quartz," *Phillips Res. Reports*, vol. 17, pp. 133-195 and 201-279, 1962.

[2] D. M. Dodd and D. B. Fraser, "The 3000-3900 cm^{-1} absorption bands and anelasticity in crystalline α-quartz," *J. Phys. Chem. Solids*, vol. 26, pp. 673-686, 1965.

[3] D. B. Fraser, "Impurity and anelasticity in crystalline quartz," *Phys. Acoust.*, W. P. Mason, Ed. New York: Academic, 1968, vol. 5, ch. 2, pp. 59-110.

[4] R. N. Brown and A. Kahan, "Optical absorption of irradiated quartz in the near IR," *J. Phys. Chem. Solids*, vol. 36, pp. 467-476, 1975.

[5] M. E. Markes and L. E. Halliburton, "Defects in synthetic quartz: Radiation-induced mobility of interstitial ions," *J. Appl. Phys.*, vol. 12, pp. 8172-8180, 1979.

[6] L. E. Halliburton, N. Koumvakalis, M. E. Markes, and J. J. Martin, "Radiation effects in crystalline SiO_2: The role of aluminum," *J. Appl. Phys.*, vol. 52, pp. 3365-3574, 1981.

[7] H. Jain and A. S. Nowick, "Radiation-induced conductivity in quartz crystals," *J. Appl. Phys.*, vol. 53, pp. 485-489, 1982.

[8] J. C. King and H. H. Sander, "Transient changes in quartz resonators following exposure to pulse ionization," *Rad. Effects*, vol. 26, pp. 203-212, 1975.

[9] P. Pellegrini, F. Euler, A. Kahan, T. M. Flanagan, and T. F. Wrobel, "Steady state and transient radiation effects in precision quartz oscillators," *IEEE Trans. Nucl. Sci.*, vol. NS-25, pp. 1267-1273, 1978.

[10] H. G. Lipson, F. Euler and A. F. Armington, "Low temperature infrared absorption of impurities in high grade quartz," in *Proc. 32nd Annu. Freq. Contr. Symp. (AFCS)*, 1978, pp. 12-23.

[11] H. G. Lipson and A. Kahan "Effects of vacuum sweeping and radiation on the defect distribution in quartz," *IEEE Trans. Nucl. Sci.*, vol. NS-31, pp. 1223-1229, 1984.

[12] H. G. Lipson and A. Kahan, "Infrared characterization of aluminum and hydrogen defect centers in irradiated quartz," *J. Appl. Phys.*, vol. 58, pp. 963-970, 1985.

[13] H. G. Lipson and F. Euler "Dose dependence of radiation-induced changes in quartz," in *Proc. 42nd AFCS*, 1988, pp. 169-175.

[14] H. G. Lipson and A. F. Armington, "Aluminum and hydroxide distribution in cultured quartz grown from $+x$ seeds," *J. Cryst. Growth*, vol. 80, pp. 51-59, 1987.

[15] A. Kahan and H. G. Lipson, "Defect centers in irradiated and swept quartz," in *Proc. 39th AFCS*, 1985, pp. 255-258.

[16] E. W. J. Mitchell and E. G. S. Paige "The anisotropic absorption of the visible bands in irradiated α-quartz," *Phil. Mag.*, vol. 46, pp. 1353-1261, 1955.

[17] A. Halperin and J. E. Ralph, "Optical studies of anisotropic color centers in germanium-doped quartz," *J. Chem. Phys.*, vol. 39, pp. 63-73, 1963.

[18] K. Nassau and B. E. Prescott, "A reinterpretation of smoky quartz," *Phys. Stat. Sol. (a)*, vol. 29, pp. 659-662, 1975.

[19] G. B. Krefft "Effects of high temperature electrolysis on the color

characteristics and OH^- absorption bands in alpha-quartz," *Rad. Effects*, vol. 26, pp. 249–259, 1975.

[20] N. Koumvakalis, "Defects in crystalline SiO_2: optical absorption of the aluminum-associated hole center," *J. Appl. Phys.*, vol. 51, pp. 5528–5532, 1980.

[21] B. K. Meyer, F. Lohse, J. M. Spaeth and J. A. Weil, "Optically detected magnetic resonance of the $[AlO_4]^0$ center in crystalline quartz," *J. Phys. C.: Solid State Phys.*, vol. 17, pp. L31–L36, 1984.

[22] H. G. Lipson, "Infrared and laser spectroscopic characterization of aluminum defects in cultured quartz," in *Proc. 40th AFCS*, 1986, pp. 63–69.

[23] H. G. Lipson and P. Zecchini, "Laser method for aluminum-hole defect distribution mapping in quartz," *Mat. Res. Soc. Symp. Proc.*, vol. 138, 1988, pp. 179–184.

Herbert G. Lipson was born in Boston, MA, on July 4, 1925. He received a B.S. degree from the Massachusetts Institute of Technology, Cambridge, MA in 1948 and an M.S. degree from Northeastern University, Boston, MA in 1964.

From 1948 to 1950 he was on the staff at Sylvania Electric Products, Bayside, NY, where he studied the sintering of metal powders and metal recrystallization. He investigated radiation effects on metals at Brookhaven National Laboratory, Patchoque, NY, between 1950 and 1951. From 1951 to 1955 he was at the Naval Research Laboratory, Washington, DC, conducting investigations on the optical properties of semiconductors and photoconductors. Between 1955 and 1958 he was a staff physicist at the Lincoln Laboratory, M.I.T., Lexington, MA, performing cyclotron resonance and magnetoplasma measurements. Since 1958, he has been at the Solid State Sciences Laboratory of the Rome Air Development Center utilizing optical absorption and fluorescence and developing laser calorimetric, laser absorption and low temperature infrared Fourier spectroscopic techniques to measure optical properties of solid state materials. His most recent work has been on defect characterization, sweeping and radiation damage effects on quartz.

Mr. Lipson is a member of the American Physical Society and the Materials Research Society.